HHS Public Access

Author manuscript

Differentiation. Author manuscript; available in PMC 2024 March 01.

Published in final edited form as:

Differentiation. 2023 ; 130: 7–15. doi:10.1016/j.diff.2022.12.001.

Fgf8 promotes survival of nephron progenitors by regulating BAX/BAKmediated apoptosis.

Matthew J. Anderson[1,*], **Salvia Misaghian**[1,*], **Nirmala Sharma**[2], **Alan O. Perantoni**[2], **Mark Lewandoski**[1,#]

[1]Genetics of Vertebrate Development Section, National Cancer Institute, National Institutes of Health, Frederick, MD 21702, USA

[2]Renal Differentiation and Neoplasia Section, Cancer and Developmental Biology Laboratory, National Cancer Institute, National Institutes of Health, Frederick, MD 21702, USA

Abstract

Fibroblast growth factors (*Fgfs*) have long been implicated in processes critical to embryonic development, such as cell survival, migration, and differentiation. Several mouse models of organ development ascribe a prosurvival requirement specifically to FGF8. Here, we explore the potential role of prosurvival FGF8 signaling in kidney development. We have previously demonstrated that conditional deletion of *Fgf8* in the mesodermal progenitors that give rise to the kidney leads to renal aplasia in the mutant neonate. Deleterious consequences caused by loss of FGF8 begin to manifest by E14.5 when massive aberrant cell death occurs in the cortical nephrogenic zone in the rudimentary kidney as well as in the renal vesicles that give rise to the nephrons. To rescue cell death in the *Fgf8* mutant kidney, we inactivate the genes encoding the pro-apoptotic factors BAK and BAX. In a wild-type background, the loss of *Bak* and *Bax* abrogates normal cell death and has minimal effect on renal development. However, in *Fgf8* mutants, the combined loss of *Bak* and *Bax* rescues aberrant cell death in the kidneys and restores some measure of kidney development: 1) the nephron progenitor population is greatly increased; 2) some glomeruli form, which are rarely observed in *Fgf8* mutants; and 3) kidney size is rescued by about 50% at E18.5. The development of functional nephrons, however, is not rescued. Thus, FGF8 signaling is required for nephron progenitor survival by regulating BAK / BAX and for subsequent steps involving, as yet, undefined roles in kidney development.

Keywords

Fibroblast growth factor; Fgf8; Kidney; Apoptosis; Cell Death

[#]Corresponding Author (lewandim@nih.gov).
[*]These authors made equal contributions

Introduction

Fibroblast growth factor (FGF) signaling is essential for the development of numerous tissues during embryonic development (reviewed in (Ornitz and Itoh, 2015)). In some tissues, a deficiency of FGF signaling causes aberrant cell death and subsequent tissue loss or malformation (Anderson et al., 2016; Boulet et al., 2004; Chi et al., 2003; Perantoni et al., 2005; Sun et al., 2002). We have previously shown that conditional inactivation of *Fgf8* in the nascent mesoderm using TCre (in TCre; $Fgf8^{flox/null}$ embryos; see Material and Methods for genetic cross), which deletes *Fgf8* before it is expressed in the kidney primordium, results in neonatal lethality as a result of kidney aplasia (Perantoni et al., 2005). This failure of kidney development appears to stem from some combination of extensive cortical and tubular cell death and a failure of *Lhx1* expression. *Lhx1* encodes a Lim-homeobox transcription factor that is expressed in the ureteric bud, nephronic pretubular aggregates, and subsequent renal vesicles (Kobayashi et al., 2005). Conditional deletion of *Lhx1* in the metanephric mesenchyme lineage results in loss of nephron structures including glomeruli and associated nephron tubules; however, NPs appear to be unaffected (Kobayashi et al., 2005; Pedersen et al., 2005). In TCre; $Fgf8^{flox/null}$ mutants, the renal vesicles fail to express *Lhx1* (Perantoni et al., 2005). Another feature of the TCre; $Fgf8^{flox/null}$ mutant kidney is widespread cell death in the cortical region where the nephron progenitors (NPs) reside as well as in the newly formed renal vesicles beginning around embryonic day 14 (E14). Therefore, *Fgf8* may be responsible for two separable actions: 1) maintaining cell survival of the NPs and 2) initiation of *Lhx1* expression in the forming renal vesicles.

Cell death occurs through numerous mechanisms, which are used for classifying this phenomenon into three main types: apoptosis, necrosis, and autophagy (reviewed (D'Arcy, 2019). Apoptosis involves an intercellular cascade that ultimately leads to fragmentation of the DNA. This cascade can be initiated intrinsically or extrinsically. The extrinsic pathway is initiated by "death ligands," such as TNFα, binding to cell surface receptors to trigger death of the cell (reviewed in (D'Arcy, 2019). The intrinsic pathway is initiated by a cytotoxic stimulus, such as withdrawal of a trophic signaling molecule, which initiates a cascade that first impacts integrity of the mitochondria. The Bcl-2 family of proteins are the major factors which interact to initiate or suppress cell death by this mitochondrial-mediated intrinsic pathway (Youle and Strasser, 2008). Tilting the balance of expression and activation of pro-death versus pro-survival Bcl-2 family members results in mitochondrial pore formation and subsequent cell death. When upstream interactions induce a cell death response, BAK and BAX oligomerize and form pores in the mitochondria. Apoptosis still occurs when either *Bak* or *Bax* are individually deleted; however, deletion of both genes blocks apoptosis (Knudson et al., 1995; Lindsten et al., 2000); thus, *Bak* and *Bax* are redundantly required for the intrinsic apoptotic pathway. To study the effects of cell death during development due to specific genetic alterations, including deletions of *Fgf3*, *Kif20b*, *Sirt6*, or *Tbx1*, cell survival has been genetically restored by the deletion of genes encoding proapoptotic factors, such as *Bak* and *Bax* or *p53* (Anderson et al., 2016; Caprio and Baldini, 2014; Ghosh et al., 2018; Little and Dwyer, 2019). In the current study, we examine the function of FGF8 signaling during embryonic kidney development and resolve its relative roles in cell survival and subsequent kidney development by inactivating the proapoptotic genes, *Bak* and *Bax.*

Results

Fgf8 is required for survival of metanephric mesenchyme

We have previously shown that kidneys in which *Fgf8* is genetically removed show extensive cell death within the cortical nephrogenic zone beginning around E14.5 (Perantoni et al., 2005). This zone includes the nephron progenitor population marked by the homeobox gene *Six2* (Self et al., 2006). To determine if cell death in TCre; $Fgf8^{flox/null}$ mutant kidneys occurs in this critical population, we evaluated the SIX2-expressing cells by immunofluorescence staining and the dying cells with Lysotracker red (Hernandez-Martinez et al., 2014). As expected, there is very little cell death in the cortical regions of E14.5 control kidneys (Figure 1A–C); however, mutants display extensive cell death in this region (Figure 1D–F). To quantify co-localized SIX2 and Lysotracker staining, spatial models were built and analyzed using Imaris software. In these models, we accounted for the nuclear localization of SIX2 immunofluorescence and the cytoplasmic location of the Lysotracker signal (Fogel et al., 2012) (Figure 1D'–F'; see "Determination of SIX2-Lysotracker double-positive cells" in Materials and Methods).

These analyses reveal that, on average, 13.4% of SIX2-positive cells are dying in *Fgf8* mutants at E14.5, compared to less than 2% of SIX2-positive cells in controls (Figure 1G). Additionally, 84.7% of dying cells within the cortex are SIX2 positive in TCre; $Fgf8^{flox/null}$. Therefore, at E14.5, when cell death is beginning in *Fgf8* mutants, a substantial number of nephron progenitors (NPs) are dying and a majority of the aberrant cell death that is observed in the *Fgf8* mutant is occurring in the SIX2-positive NPs.

Genetic abrogation of cell death does not adversely affect kidney development

One hypothesis for why the kidney fails to develop beyond a rudimentary state in the *Fgf8* mutant is that the NPs and their derivatives are dying, thereby preempting nephron formation. To explore this hypothesis, we attempted to restore cell survival by inactivating the redundantly required pro-apoptotic pathway genes *Bak* and *Bax* (Fletcher and Huang, 2008; Takeuchi et al., 2005; Westphal et al., 2014). Homozygous null *Bak* mutants are normal and viable, but a majority of the homozygous *Bax* mutants die perinatally (Lindsten et al., 2000). Combined loss of *Bak* and *Bax* resulted in defects in the patterning of certain tissues, such as interdigital webbing and imperforate vagina; however, the kidneys were reported to be overtly normal (Lindsten et al., 2000). Therefore, we utilized *Bak* and *Bax* null alleles in the cross illustrated in Figure 2A to produce the three resultant genotypes of interest at the expected frequency of 1 in 8. The "most wildtype" genotype produced from this cross, hereafter called "*Control Bak*", is lacking one allele of *Fgf8* in the TCre lineage and is homozygous null for *Bak*. The simplest genotype lacking Fgf8 produced from this cross, hereafter called "*Fgf8 mutant*", lacks both alleles of *Fgf8* in the TCre lineage and is homozygous null for *Bak*. Lastly, we designated the genotype lacking *Fgf8* in the TCre lineage and also homozygous null for both Bak and Bax, "*Rescued Fgf8 mutant*" (Figure 2A).

To determine if loss of *Bak* has any consequence on kidney development, we analyzed the morphology and size of wild-type *Bak* kidneys in comparison with "*Control Bak*" kidneys

and found no changes (Supplemental Fig 1A–J, U), validating the use of the *Control Bak* kidneys as littermate controls that have normal kidney development. Likewise, the littermate *Fgf8 mutant* genotype was also homozygous null for *Bak*; however, we also found no discernible changes in cell death, morphology, or size of the kidneys when compared to TCre; $Fgf8^{flox/null}$ mutants (Supplemental Fig 1K–U). We therefore used these *Fgf8 mutant* kidneys for comparison as littermate controls with the *Fgf8* loss-of-function kidney defect for the remainder of this study.

We then asked whether homozygous loss of both *Bak* and *Bax* impacts kidney development independent of *Fgf8*. Therefore, we scrutinized embryonic kidneys from animals containing one wild-type allele of *Fgf8* in the TCre lineage and null for both *Bak* and *Bax* and compared them with littermate *Control Bak* kidneys (therefore the only genetic difference is whether they are wild-type or null homozygous for *Bax*). These Control kidneys lacking both *Bak* and *Bax* were overtly normal by gross examination as previously noted (Supplemental Fig 2A, B)(Lindsten et al., 2000). However, we noted they were 9.3% smaller in length than *Control Bak* kidneys (Supplemental Fig 2C). This change in length does not impact the number of nephrons on the basis of glomeruli counts or histological appearance of the kidney (Supplemental Fig 2D–F). Therefore we concluded this small size reduction did not diminish the utility of deleting *Bak* and *Bax* to interrogate the role of cell death in the phenotype caused by *Fgf8* loss in the kidney.

Restored cell survival in *Fgf8 mutants* partially rescues kidney development

Having thoroughly characterized kidney development in our control littermate genotypes, we then examined the outcome of homozygous deletion of *Bak* and *Bax* to rescue the aberrant cell death in the *Fgf8 mutant* cortical regions. *Fgf8 mutants* have extensive cell death in the cortical regions and renal vesicles at E14.5 (Figure 2E compare to B), whereas *Rescued Fgf8 mutants* have no cell death in the cortical nephrogenic zone (Figure 2H). Compared to *Fgf8 mutants*, *Rescued Fgf8 mutant* kidneys exhibit an increase in size at E18.5 as measured by length (Figure 2I compared to 2K, quantified in 2F). However, these *Rescued Fgf8 mutant* kidneys are still significantly smaller than *Control Bak* kidneys (Figure 2C and 2K). *Rescued Fgf8 mutant* kidneys also displayed two histological changes: 1) an accumulation of blastemal-like mesenchymal cells in the cortical region (Figure 2J, black bracket) and 2) patent glomeruli (Figure 2J, green asterisks). Both observations are analyzed in greater detail in the following sections.

Restoring Survival Rescues Nephron Progenitor Loss

To explore the apparent thickening of the cortical mesenchyme, we first stained kidneys with an antibody for SIX2 to detect nephron progenitors in the cap mesenchyme at E14.5, E16.5, and E18.5. *Fgf8 mutants* exhibited a normal pattern of SIX2 expression at E14.5. However by E16.5, NPs were markedly diminished, and by E18.5, almost no SIX2 positive cells were evident (Figure 3D–F). *Rescued Fgf8 Mutants,* which display no lysotracker signal (Figure 2H), had normal expression of SIX2 at E14.5 and E16.5, and at E18.5 had a large number of SIX2-positive cells in the cortical mesenchyme (Figure 3G–I), although the organization of SIX2-positive NPs was aberrant, i.e., they were less compact and individual cells were more diffusely scattered at E18.5 (compare Figure 3I with 3C).

To further examine the restoration of the NPs, we performed immunohistochemistry for a panel of MM markers. CITED1 labels a subset of the SIX2-positive NP population and is downregulated as these cells begin a mesenchymal-epithelial transition (Figure 4B) (Boyle et al., 2007). PAX2 is robustly expressed in the cap mesenchyme and renal vesicle and to a lesser extent the ureteric bud (UB) (Figure 4C) (Brophy et al., 2001). SALL1 is also highly expressed in cap mesenchyme and renal vesicle and at lower levels in stroma and UB (Figure 4D) (Nishinakamura et al., 2001). We saw a similar trend in loss of MM markers as previously described (Perantoni et al., 2005); SIX2, CITED1, PAX2, and SALL1 expression is substantially reduced or lost in *Fgf8 mutants* (Figure 4E–H). Furthermore, all of these markers are restored in the MM of *Rescued Fgf8 mutants* (Figure 4K–N). These observations were confirmed by RT-qPCR analyses, in which the levels of *Six2*, *Cited1,* and *Sall1* expression were significantly increased in *Rescued Fgf8 mutants* compared to *Fgf8 mutants* (Figure 4M). *Pax2* expression was restored to normal levels in *Rescued Fgf8 mutants*. This change, however, was found not to be significant when compared with expression in *Fgf8* mutants (Figure 4M). *Foxd1*, a marker of the stromal progenitor population, was unchanged among all genotypes (Figure 4M) (Hatini et al., 1996). Therefore, the restoration of cell survival in kidneys lacking *Fgf8* is sufficient to restore the MM progenitor populations that sustain nephrogenesis.

Restoring Survival Does Not Rescue Nephron Formation

Histologically, we observed glomerular-like structures in *Rescued Fgf8 mutants* (Figure 2J). To confirm their identity, we immunolabeled E18.5 kidneys with an antibody for NEPHRIN, a marker of podocytes within glomeruli (Kestila et al., 1998). *Fgf8 mutant* kidneys rarely revealed any NEPHRIN-positive glomeruli (Figure 5B); however, *Rescued Fgf8 mutants* contained some NEPHRIN-positive glomeruli (Figure 5C), although fewer than *Control Bak* kidneys (Figure 5A). Quantification of NEPHRIN-positive glomeruli showed a significant increase in *Rescued Fgf8 mutant* kidneys (7.8 glomeruli per section) compared to *Fgf8 mutant* kidneys (1.45 glomeruli per section); however, *control Bak* kidneys had nearly 4-fold more glomeruli (29.2 glomeruli per section). Therefore, restoration of cell survival had a marginal, albeit statistically significant, effect on glomerular number.

The glomeruli of *Rescued Fgf8 mutants* appeared large and cystic (Figure 5C, asterisk), suggesting that these glomeruli lacked a patent tubular connection for drainage and waste excretion. We therefore examined whether there was any rescue of tubule formation when cell survival was restored in *Fgf8 mutants*. To accomplish this, we utilized fluorescent whole mount *in situ* hybridization chain reaction (HCR) using probes against *Slc5a1*, a marker of the proximal convoluted tubule (Vallon et al., 2011), and *Slc12a1*, a marker of the ascending limb of the loop of Henle (Gamba et al., 1994; Payne and Forbush, 1994). *Control Bak* kidneys had clear labeling of *Slc5a1* and *Slac12a1* in each structure (Figure 5E), and, as expected, *Fgf8 mutants* had neither structure (Figure 5F). *Rescued Fgf8 mutants* also yielded no labeling from either marker, indicating that they too lack these renal tubules and thus functional nephrons (Figure 5G). Therefore, restoring cell survival in *Fgf8 mutants* did not rescue tubule formation.

LHX1 is a LIM homeobox transcription factor that is required for nephron formation, specifically tubule formation, and is expressed in pretubular aggregates, renal vesicles, and to a lesser extent, the UB (Kobayashi et al., 2005). We have previously shown that *Fgf8 mutants* lack *Lhx1* expression in pretubular aggregates and that *Lhx1* expression can be induced by FGF8 *ex vivo* (Perantoni et al., 2005). We therefore examined LHX1 expression in mutants when cell survival is restored. As expected, LHX1 expression in the pretubular aggregates was present in littermate *Control Bak* kidneys and absent in *Fgf8 mutants* kidneys (Figure 5H and I). *Rescued Fgf8 mutants* also had no pretubular aggregate expression of LHX1 (Figure 5J). Given the crucial role of LHX1 in tubulogenesis, this finding is consistent with the lack of tubules in *Rescued Fgf8 mutants* (Figure 5G).

In conclusion, blocking apoptotic cell death in *Fgf8* mutant kidneys can partially rescue kidney development, in which NPs are sustained, more glomerular-like structures appear, but subsequent nephron formation fails. These observations show that indeed FGF8 signals to block apoptosis in the cortical mesenchyme but also functions to promote subsequent nephronic development. It is possible that this latter signaling is necessary to induce *Lhx1* expression in the early stages of renal vesicle formation.

Discussion

Here we analyze embryonic development in mouse kidneys that lack *Fgf8* in which we have restored cell survival through the genetic deletion of *Bak* and *Bax.* Our analysis is founded on the careful examination of control littermate kidneys; *Bak* and *Bax* deletion (in *Fgf8* wildtype kidneys) results in no overt consequence on renal development except for a slight decrease in kidney size. Our data show that FGF8 prevents nephron progenitor apoptosis and maintains *Lhx1* expression. Additionally, FGF8 may play a role in regulating NP cell migration.

FGF8 prevents nephron progenitor apoptosis.

FGFs have been shown to promote cell survival in the developing lens, teeth, cranial neural crest, tail bud, and limbs (Anderson et al., 2016; Chow et al., 1995; Montero et al., 2001; Ray et al., 2020; Vaahtokari et al., 1996). The aberrant cell death in developing kidneys, caused by *Fgf8* loss, is rescued when the intrinsic apoptotic pathway is abrogated, demonstrating that FGF8 maintains cell survival in a BAK/BAX-dependent manner. BAK and BAX act near the end of a cascade of activation events to permeabilize the mitochondrial outer membrane and release apoptotic factors (Fletcher and Huang, 2008; Westphal et al., 2014). FGFs signal through multiple pathways (Brewer et al., 2016) that potentially regulate different nodes of this cell survival/death pathway. For example, FGF signals have been shown to engage the PI3K/AKT pathway to phosphorylate BAD, resulting in antiapoptotic activity upstream of BAK/BAX (Miho et al., 1999; Wente et al., 2006). Another candidate for regulation by FGF-signaling is BIM. Deletion of one *Bim* allele, which encodes an apoptosis initiator that directly activates BAK/BAX (Chipuk and Green, 2008; Czabotar et al., 2014), will partially rescue aberrant cell death that underlie craniofacial defects that are due to the loss of *Fgfr1* and *Fgfr2* (Ray et al., 2020). Our model

for genetically rescuing cell death in the *Fgf8* mutant kidney presents a future opportunity to explore the role of FGFs in pro-survival signaling *in vivo*.

FGF8 maintains Lhx1 expression

In addition to extensive cortical cell death, kidneys lacking *Fgf8* also fail to express *Lhx1*(Perantoni et al., 2005). Pretubular aggregates form in *Lhx1*-deficient embryos but stall at renal vesicle formation and subsequently degenerate (Kobayashi et al., 2005). In the *Rescued Fgf8 mutant*, nephron progenitors are present, however renal vesicle formation similarly arrests shortly after initiation. Restoration of cell survival does not restore LHX1 protein expression in *Fgf8 mutant* kidneys. Therefore, in addition to providing a pro-survival signal, FGF8 is likely also required for inducing or maintaining *Lhx1* expression. Deficient *Lhx1* expression could explain the lack of renal vesicle maturation and subsequent failure of nephron formation in the *Rescued Fgf8 mutant*. The renal vesicles that are found in the *Rescued Fgf8 mutant* at E18.5 are likely formed prior to E14.5 and would undergo apoptosis in the absence of *Fgf8,* if apoptosis were not blocked. However, due to deficient *Lhx1* expression, these primitive renal vesicles fail to elongate and form mature nephrons. It is possible that aberrant cell death is a function of *Lhx1* loss. Although apoptosis is yet to be analyzed in *Lhx1* mutant kidneys, like *Fgf8* mutant kidneys, they are smaller (Kobayashi et al., 2005). Moreover, *Lhx1* loss has been shown to cause increased apoptosis in the Mü llerian duct epithelium (Huang et al., 2014).

The initial formation of renal vesicles prior to E14.5 in the Fgf8 mutant is likely driven by redundant signaling from FGF9 and FGF20. *Fgf9* is expressed in the UB and weakly in the MM, while *Fgf20* is found in the MM and early renal vesicle (Barak et al., 2012). When *Fgf9* and *Fgf20* are lost, there is a rapid depletion of MM between E11.5 and E12.5 involving apoptosis of this tissue (Barak et al., 2012). *Fgf9* and *Fgf20* are however not sufficient for sustaining renal vesicle development beyond E14.5, at which time *Fgf8* is required for this process. Therefore, these three FGF family members may act redundantly over the course of kidney formation.

FGF8 may regulate NP cell migration

In the absence of *Fgf8* (and with cell survival restored), renal progenitor cells, as labeled by SIX2, accumulate in the cortical nephrogenic zone. One explanation for this defect in *Rescued Fgf8 mutants* is that FGF8 may function in renal development by regulating NP cell migration during renal vesicle formation. This speculation is consistent with the observation that FGF signaling regulates cellular migration in several embryonic tissues (Bottcher and Niehrs, 2005; Kumar et al., 2021), including the vertebrate nephric duct (Attia et al., 2015).

Migration of NP cells is an essential process in both their maintenance as well as their differentiation (Lawlor et al., 2019). The cap mesenchyme (CM) cells exist in a niche surrounding the distal end of cortical uretic bud tips. Migration of CM is driven by a combination of attractive and repulsive cues from the surrounding interstitial cells and from uretic bud tips (Combes et al., 2016). It is thought that cells must migrate out of this region to downregulate progenitor maintenance genes and begin initiating differentiation programs (Lawlor et al., 2019).

Starting at E11.5, *Fgf8* is expressed in a ring below the branching UB, and thereafter within the pretubular aggregates and newly formed renal vesicles at E14.5 NPs (Grieshammer et al., 2005; Perantoni et al., 2005) and therefore may encode an attractant activity for cortical NPs and migrating CM cells. Therefore, it is logical that a failure in migration of cortical nephron progenitor descendants would lead to an accumulation of SIX2-positive cells in the nephrogenic zone, as we observe in *Rescued Fgf8 mutants*. Alteratively, defects in homeostasis may also explain this aberrant accumulation of progenitors. Future time-lapse imaging analysis of these mutant cells will yield insightful data clarifying these ideas.

WNT signaling has been shown to be key in regulating CM migration, specifically WNT9b and WNT11 (O'Brien et al., 2018). *Wnt11* inactivation causes a failure in CM migration and subsequent disorganization, similar to the *Rescued Fgf8 mutant* phenotype. FGFs and WNTs interact in multiple tissues to affect tissue morphogenesis (Naiche et al., 2011; ten Berge et al., 2008; Yin et al., 2008), and it is therefore possible that the failed CM migration that occurs in the *Rescued Fgf8 mutant* is due to loss of WNT-driven migration.

FGF8 signaling within the kidney mesenchyme functions to support cell survival by blocking apoptosis, instructing cell fate, and possibly regulating cell migration, all of which are related to basic hallmarks of cancer development and progression (Hanahan and Weinberg, 2011). Furthermore, *Lhx1* and *Six2,* both regulated by FGF8, are implicated in renal cancer development (Dormoy et al., 2011; Pierce et al., 2014). Further investigation of the mechanism of FGF8 signaling to control the expression of the genes and developmental processes will not only impact our understanding of the role of *Fgf8* in kidney development, but also lead to insights regarding cancer.

Methods and Materials

Alleles, Genotyping, and Kidney Dissection

All mice were kept on a mixed background. PCR-genotyping for each allele was performed using the following primer combinations, *Fgf8flox*(Meyers et al., 1998) (5'-GG TCT TTC TTA GGG CTA TCC AAC and 5'-GCT CAC CTT GGC AAT TAG CTT C) *Fgf8Δ*(Meyers et al., 1998) (5'-CCA GAG GTG GAG TCT CAG GTC C and 5'-GCA CAA CTA GAA GGC AGC TCC C), *Bak*(Lindsten et al., 2000) (5'- GGC TCT TCA CCC CTT ACA TCA G, 5'- GTT TAG CGG GCC TGG CAA CG, and 5'- GCA GCG CAT CGC CTT CTA TC), *BaxΔ*(Lindsten et al., 2000) (5'- CAA CTC CTA CCG CAA GTC CTG G and 5'- GAA CCC TAG GAC CCC TCC G), *BaxWT* (5'- TGC CGA ACT GGG CAC TGT TG and 5'- GTC CTG GGG AAT GTG GAC TG), TCre(Perantoni et al., 2005) (5'- GGG ACC CAT TTT TCT CTT CC and 5'-CCA TGA GTG AAC GAA CCT GG). Embryos where dissected on the noted embryonic day in chilled PBS and kidneys where removed from the embryo and fixed in 4% paraformaldehyde at 4°C, rocking overnight. The following day, kidneys where washed in PBS, then dehydrated, stepwise, into 100% methanol and stored at −20 °C.

Wholemount Lyostracker Staining

E14.5 and E16.5 kidneys were dissected in 37° C Hanks BSS without phenol red with Mg^{+2} and Ca^{+2}. The isolated kidneys were placed in 5 ml Hanks and 25 ul LysoTracker Red

(Invitrogen) and cultured at 37° C for 30 minutes, then rinsed in Hanks and fixed in 4% paraformaldehyde at room temperature for 30 minutes. They were then rinsed with PBS, dehydrated into 100% methanol and stored at - 20° C, until time of imaging.

Lysotracker Staining and Six2 Immunohistochemistry

Lysotracker staining was performed as noted above. Then kidneys were rehydrated and rinsed in 1% Triton in PBS for 10 minutes at room temperature. The tissues were then blocked in 5% goat serum in 1% Triton X-100 PBS for two hours at room temperature and incubated in anti-SIX2 (Proteintech: 11562–1-AP, 1:50) overnight at 4°C while rocking. The following day, kidneys were then washed in 1% Triton X-100 in PBS 3 × 10 minutes at room temperature and incubated with Alexa Fluor 488 conjugated goat anti-rabbit IgG (Thermo Fisher: A-11008, 1:250) and 0.5ug/mL DAPI overnight at 4°C. Kidneys were then washed with 1% Triton X-100 in PBS 3 × 10 minutes at room temperature, embedded in 7% Low Melting Point Agarose, and 80 μm sections were cut using a vibratome.

Immunohistochemistry on Paraffin Sections

Kidneys were moved into 100% ethanol, then into Citrisolv, followed by two changes of melted paraffin wax, before final positioning in paraffin. Sections (8um) where cut from the paraffin blocks, and deparaffinized using Citrisolv reagent. Sections where blocked with 5% goat serum in 1% Triton X-100 PBS for two hours at room temperature and incubated in primary antibody overnight at 4°C in a humidified chamber. Slides where then washed 3× 20 minutes in 1% Triton X-100 PBS at room temperature and incubated with the appropriate secondary antibody and 0.5ug/mL DAPI overnight at 4°C in a humidified chamber. Slides were washed 3× 20 minutes in 1% Triton X-100 PBS at room temperature and tissues preserved under coverslips using AquaPoly/Mount (Polysciences, 18606). The following primary and secondary antibodies at indicated concentrations were used: rabbit polyclonal Six2 antibody (Proteintech, 1:50), rabbit polyclonal Cited1 antibody (Neomarkers, 1:50), rabbit polyclonal Pax2 antibody (Invitrogen antibodies, 1:50), rabbit polyclonal Sall1 antibodies (abcam, 1:50), and guinea pig polyclonal Nephrin antibodies (Progen, 1:50), Alexa Fluor 488 conjugated goat anti-rabbit IgG (Thermo Fisher: A-11008, 1:250), Alexa Fluor 647 conjugated goat anti-guinea pig IgG (Thermo Fisher: A-21450, 1:250).

Confocal Imaging and Image Analysis

All fluorescent images were taken using an Olympus FV1000 with a 20x UPlanApo objective (NA: 0.70) with 3X-Kalman averaging. Images where processed using FIJI software to generate Max Intensity Projections. Identical intensity ranges where used between compared samples.

Determination of SIX2-Lysotracker double-positive cells

Spatial models were generated using Imaris software (Imaris V9.2.1, Bitplane Inc), to analyze Lysotracker-SIX2 double positive cells. This was done to account for nuclear-localized SIX2 staining and lysotracker staining, which may be localized anywhere within the cell REF), since standard pixel-based colocalization cannot accurately identify double positive cells. Within the Imaris software, the “spot” modeling tool was used to generate

spot features for each channel (SIX2 and Lysotracker). Because the diameter and intensity of SIX2 positive cells varied, three different spot models were created: 7 μm XY diameter and 7 μm Z diameter using a minimum sum intensity threshold of 1.25 e5; 2 μm XY diameter and 4 μm Z diameter using a minimum sum intensity threshold of 5800 and upper threshold of 1.50 e4; and 3 um XY diameter and 4 um Z diameter using a minimum sum intensity threshold of 8000 and upper threshold of 1.50 e5. Redundant spots generated from the three models that labeled the same SIX2 positive cells were eliminated from the analysis by colocalizing spots that were within 5 um from each other, and only analyzing those that were unique (omitting the redundant spots from the analysis). Each SIX2 spot labeled one nucleus and therefore represents one cell. For spot modeling of the Lysotracker positive signal a 3.5 um XY diameter and 8 um Z diameter and minimum sum intensity of 1.00 e4 was used to generate spots.

To exclusively analyze Lysotracker staining in the cortical region (and not renal vesicle or medullary cell death) the Imaris “surface” tool was utilized to generate a volumetric model. Surface models were generated based on SIX2 positivity with surface detail of 2 um and a low absolute intensity threshold of 1200, to encompass all SIX2 positive cells. All lysotracker spots within 10 um of the Six2 positive surface model were considered cortical and used for colocalization with spots modeling SIX2 positive cells. The threshold for colocalization between SIX2 and lysotracker spots was 5 um. Colocalization of one SIX2 spot with multiple lysotracker spots or vice versa was manually checked to ensure single colocalized pairs; in the event of multiple colocalizations, only one of each class of spot was counted to be colocalized.

Hybridization Chain Reaction whole mount *in situ*

Hybridization Chain Reaction whole mount *in situ* split initiator probes (V3.0) were designed and synthesized by Molecular Instruments, Inc. Staining was carried out as previously described (Anderson et al., 2020).

RT-qPCR

Both kidney rudiments from each embryo were isolated at the indicated ages, frozen on dry ice, and stored at −80°C, while the embryos were being genotyped. Total RNA from 10–15 pairs of metanephroi with the same genotypes was purified using TRIzol reagent (Invitrogen cat# 15596026). Following extraction, RNA preparations were dissolved in 10 μl DEPC-treated distilled water. For RT-PCR, random hexamer primers were used to generate cDNA with a Verso kit from Thermo Scientific cat #AB1453/B. For this, total RNA was incubated at 42°C for 30 min and 95°C for 2 min. For quantitative PCR, 1 μl cDNA was used in a 20 μl reaction mixture with a Bio-Rad SsoFast EvaGreen super mix Kit (cat# 1725201) and 3μM gene-specific primers in a Bio Rad CFX96 real-time PCR detection system. Incubation conditions typically consisted of 45 cycles (3min 95°c, 5s 95°c 5s 65°c), depending upon primer optimal annealing temperatures. Relative levels of gene expression were calculated using ΔCq values and normalized to *GAPDH* expression. Primers for each cDNA gene-specific reaction were as follows: *Cited1* (5’ - AAT GTG TCC GTC GTG GAT CTG - 3’ and 5’ - CTG CTT CAC CAC CTT CTT GAT GT - 3’)*;FoxD1* (5’ – TCG CTC TGT CTT GGC ACT AGG A - 3’ and 5’ – ACG CCT GGA CCT GAG AAT CTC TAC -

3’);; *GAPDH* (5’ - AAT GTG TCC GTC GTG GAT CTG - 3’ and 5’ - CTG CTT CAC CAC CTT CTT GAT GT - 3’); *Pax2* (5’- AGG CAT CAG AGC ACA TCA AAT CAG - 3’ and 5’- GGG TTG GCC GAT GCA GAT AG - 3’); *Sall1* (5’ - TGT CAA GTT CCC AGA AAT GTT CCA and 5’ - ATG CCG CCG TTC TGA ATG A - 3’); and *Six2* (5’ - GCA ACT TCC GCG AGC TCT AC - 3’ and 5’ - GCC TTG AGC CAC AAC TGC TG - 3’).

Supplementary Material

Refer to Web version on PubMed Central for supplementary material.

Acknowledgements

We thank Patricia Abete-Luzi, Christian Bonatto, Michael Boylan, Cindy Elder, and Erika Truffer for technical assistance or critical reading of the manuscript.

Funding

This work was supported by the Center for Cancer Research of the Intramural Research Program of the National Institutes of Health through the National Cancer Institute.

References

Anderson MJ, Magidson V, Kageyama R, Lewandoski M, 2020. Fgf4 maintains Hes7 levels critical for normal somite segmentation clock function. Elife 9.

Anderson MJ, Schimmang T, Lewandoski M, 2016. An FGF3-BMP Signaling Axis Regulates Caudal Neural Tube Closure, Neural Crest Specification and Anterior-Posterior Axis Extension. PLoS Genet 12, e1006018.

Attia L, Schneider J, Yelin R, Schultheiss TM, 2015. Collective cell migration of the nephric duct requires FGF signaling. Dev Dyn 244, 157–167. [PubMed: 25516335]

Barak H, Huh SH, Chen S, Jeanpierre C, Martinovic J, Parisot M, Bole-Feysot C, Nitschke P, Salomon R, Antignac C, Ornitz DM, Kopan R, 2012. FGF9 and FGF20 maintain the stemness of nephron progenitors in mice and man. Dev Cell 22, 1191–1207. [PubMed: 22698282]

Bottcher RT, Niehrs C, 2005. Fibroblast growth factor signaling during early vertebrate development. Endocr Rev 26, 63–77. [PubMed: 15689573]

Boulet AM, Moon AM, Arenkiel BR, Capecchi MR, 2004. The roles of Fgf4 and Fgf8 in limb bud initiation and outgrowth. Dev Biol 273, 361–372. [PubMed: 15328019]

Boyle S, Shioda T, Perantoni AO, de Caestecker M, 2007. Cited1 and Cited2 are differentially expressed in the developing kidney but are not required for nephrogenesis. Dev Dyn 236, 2321–2330. [PubMed: 17615577]

Brewer JR, Mazot P, Soriano P, 2016. Genetic insights into the mechanisms of Fgf signaling. Genes Dev 30, 751–771. [PubMed: 27036966]

Brophy PD, Ostrom L, Lang KM, Dressler GR, 2001. Regulation of ureteric bud outgrowth by Pax2-dependent activation of the glial derived neurotrophic factor gene. Development 128, 4747–4756. [PubMed: 11731455]

Caprio C, Baldini A, 2014. p53 Suppression partially rescues the mutant phenotype in mouse models of DiGeorge syndrome. Proc Natl Acad Sci U S A 111, 13385–13390.

Chi CL, Martinez S, Wurst W, Martin GR, 2003. The isthmic organizer signal FGF8 is required for cell survival in the prospective midbrain and cerebellum. Development 130, 2633–2644.

Chipuk JE, Green DR, 2008. How do BCL-2 proteins induce mitochondrial outer membrane permeabilization? Trends Cell Biol 18, 157–164. [PubMed: 18314333]

Chow RL, Roux GD, Roghani M, Palmer MA, Rifkin DB, Moscatelli DA, Lang RA, 1995. FGF suppresses apoptosis and induces differentiation of fibre cells in the mouse lens. Development 121, 4383–4393. [PubMed: 8575338]

Combes AN, Lefevre JG, Wilson S, Hamilton NA, Little MH, 2016. Cap mesenchyme cell swarming during kidney development is influenced by attraction, repulsion, and adhesion to the ureteric tip. Dev Biol 418, 297–306. [PubMed: 27346698]

Czabotar PE, Lessene G, Strasser A, Adams JM, 2014. Control of apoptosis by the BCL-2 protein family: implications for physiology and therapy. Nat Rev Mol Cell Biol 15, 49–63. [PubMed: 24355989]

D'Arcy MS, 2019. Cell death: a review of the major forms of apoptosis, necrosis and autophagy. Cell Biol Int 43, 582–592. [PubMed: 30958602]

Dormoy V, Beraud C, Lindner V, Thomas L, Coquard C, Barthelmebs M, Jacqmin D, Lang H, Massfelder T, 2011. LIM-class homeobox gene Lim1, a novel oncogene in human renal cell carcinoma. Oncogene 30, 1753–1763. [PubMed: 21132009]

Fletcher JI, Huang DC, 2008. Controlling the cell death mediators Bax and Bak: puzzles and conundrums. Cell Cycle 7, 39–44. [PubMed: 18196961]

Fogel JL, Thein TZ, Mariani FV, 2012. Use of LysoTracker to detect programmed cell death in embryos and differentiating embryonic stem cells. J Vis Exp.

Gamba G, Miyanoshita A, Lombardi M, Lytton J, Lee WS, Hediger MA, Hebert SC, 1994. Molecular cloning, primary structure, and characterization of two members of the mammalian electroneutral sodium-(potassium)-chloride cotransporter family expressed in kidney. J Biol Chem 269, 17713–17722.

Ghosh S, Wong SK, Jiang Z, Liu B, Wang Y, Hao Q, Gorbunova V, Liu X, Zhou Z, 2018. Haploinsufficiency of Trp53 dramatically extends the lifespan of Sirt6-deficient mice. Elife 7.

Grieshammer U, Cebrian C, Ilagan R, Meyers E, Herzlinger D, Martin GR, 2005. FGF8 is required for cell survival at distinct stages of nephrogenesis and for regulation of gene expression in nascent nephrons. Development 132, 3847–3857. [PubMed: 16049112]

Hanahan D, Weinberg RA, 2011. Hallmarks of cancer: the next generation. Cell 144, 646–674. [PubMed: 21376230]

Hatini V, Huh SO, Herzlinger D, Soares VC, Lai E, 1996. Essential role of stromal mesenchyme in kidney morphogenesis revealed by targeted disruption of Winged Helix transcription factor BF-2. Genes Dev 10, 1467–1478. [PubMed: 8666231]

Hernandez-Martinez R, Cuervo R, Covarrubias L, 2014. Detection of cells programmed to die in mouse embryos. Methods Mol Biol 1092, 269–289. [PubMed: 24318827]

Huang CC, Orvis GD, Kwan KM, Behringer RR, 2014. Lhx1 is required in Mullerian duct epithelium for uterine development. Dev Biol 389, 124–136. [PubMed: 24560999]

Kestila M, Lenkkeri U, Mannikko M, Lamerdin J, McCready P, Putaala H, Ruotsalainen V, Morita T, Nissinen M, Herva R, Kashtan CE, Peltonen L, Holmberg C, Olsen A, Tryggvason K, 1998. Positionally cloned gene for a novel glomerular protein--nephrin--is mutated in congenital nephrotic syndrome. Mol Cell 1, 575–582. [PubMed: 9660941]

Knudson CM, Tung KS, Tourtellotte WG, Brown GA, Korsmeyer SJ, 1995. Bax-deficient mice with lymphoid hyperplasia and male germ cell death. Science 270, 96–99. [PubMed: 7569956]

Kobayashi A, Kwan KM, Carroll TJ, McMahon AP, Mendelsohn CL, Behringer RR, 2005. Distinct and sequential tissue-specific activities of the LIM-class homeobox gene Lim1 for tubular morphogenesis during kidney development. Development 132, 2809–2823. [PubMed: 15930111]

Kumar V, Goutam RS, Park S, Lee U, Kim J, 2021. Functional Roles of FGF Signaling in Early Development of Vertebrate Embryos. Cells 10.

Lawlor KT, Zappia L, Lefevre J, Park JS, Hamilton NA, Oshlack A, Little MH, Combes AN, 2019. Nephron progenitor commitment is a stochastic process influenced by cell migration. Elife 8.

Lindsten T, Ross AJ, King A, Zong WX, Rathmell JC, Shiels HA, Ulrich E, Waymire KG, Mahar P, Frauwirth K, Chen Y, Wei M, Eng VM, Adelman DM, Simon MC, Ma A, Golden JA, Evan G, Korsmeyer SJ, MacGregor GR, Thompson CB, 2000. The combined functions of proapoptotic Bcl-2 family members bak and bax are essential for normal development of multiple tissues. Mol Cell 6, 1389–1399. [PubMed: 11163212]

Little JN, Dwyer ND, 2019. p53 deletion rescues lethal microcephaly in a mouse model with neural stem cell abscission defects. Hum Mol Genet 28, 434–447. [PubMed: 30304535]

Meyers EN, Lewandoski M, Martin GR, 1998. An Fgf8 mutant allelic series generated by Cre- and Flp-mediated recombination. Nat Genet 18, 136–141. [PubMed: 9462741]

Miho Y, Kouroku Y, Fujita E, Mukasa T, Urase K, Kasahara T, Isoai A, Momoi MY, Momoi T, 1999. bFGF inhibits the activation of caspase-3 and apoptosis of P19 embryonal carcinoma cells during neuronal differentiation. Cell Death Differ 6, 463–470. [PubMed: 10381633]

Montero JA, Ganan Y, Macias D, Rodriguez-Leon J, Sanz-Ezquerro JJ, Merino R, Chimal-Monroy J, Nieto MA, Hurle JM, 2001. Role of FGFs in the control of programmed cell death during limb development. Development 128, 2075–2084. [PubMed: 11493529]

Naiche LA, Holder N, Lewandoski M, 2011. FGF4 and FGF8 comprise the wavefront activity that controls somitogenesis. Proc Natl Acad Sci U S A 108, 4018–4023. [PubMed: 21368122]

Nishinakamura R, Matsumoto Y, Nakao K, Nakamura K, Sato A, Copeland NG, Gilbert DJ, Jenkins NA, Scully S, Lacey DL, Katsuki M, Asashima M, Yokota T, 2001. Murine homolog of SALL1 is essential for ureteric bud invasion in kidney development. Development 128, 3105–3115. [PubMed: 11688560]

O'Brien LL, Combes AN, Short KM, Lindstrom NO, Whitney PH, Cullen-McEwen LA, Ju A, Abdelhalim A, Michos O, Bertram JF, Smyth IM, Little MH, McMahon AP, 2018. Wnt11 directs nephron progenitor polarity and motile behavior ultimately determining nephron endowment. Elife 7.

Ornitz DM, Itoh N, 2015. The Fibroblast Growth Factor signaling pathway. Wiley Interdiscip Rev Dev Biol 4, 215–266. [PubMed: 25772309]

Payne JA, Forbush B 3rd, 1994. Alternatively spliced isoforms of the putative renal Na-K-Cl cotransporter are differentially distributed within the rabbit kidney. Proc Natl Acad Sci U S A 91, 4544–4548. [PubMed: 7514306]

Pedersen A, Skjong C, Shawlot W, 2005. Lim 1 is required for nephric duct extension and ureteric bud morphogenesis. Dev Biol 288, 571–581. [PubMed: 16216236]

Perantoni AO, Timofeeva O, Naillat F, Richman C, Pajni-Underwood S, Wilson C, Vainio S, Dove LF, Lewandoski M, 2005. Inactivation of FGF8 in early mesoderm reveals an essential role in kidney development. Development 132, 3859–3871. [PubMed: 16049111]

Pierce J, Murphy AJ, Panzer A, de Caestecker C, Ayers GD, Neblett D, Saito-Diaz K, de Caestecker M, Lovvorn HN 3rd, 2014. SIX2 Effects on Wilms Tumor Biology. Transl Oncol 7, 800–811. [PubMed: 25500091]

Ray AT, Mazot P, Brewer JR, Catela C, Dinsmore CJ, Soriano P, 2020. FGF signaling regulates development by processes beyond canonical pathways. Genes Dev 34, 1735–1752. [PubMed: 33184218]

Self M, Lagutin OV, Bowling B, Hendrix J, Cai Y, Dressler GR, Oliver G, 2006. Six2 is required for suppression of nephrogenesis and progenitor renewal in the developing kidney. EMBO J 25, 5214–5228. [PubMed: 17036046]

Sun X, Mariani FV, Martin GR, 2002. Functions of FGF signalling from the apical ectodermal ridge in limb development. Nature 418, 501–508. [PubMed: 12152071]

Takeuchi O, Fisher J, Suh H, Harada H, Malynn BA, Korsmeyer SJ, 2005. Essential role of BAX,BAK in B cell homeostasis and prevention of autoimmune disease. Proc Natl Acad Sci U S A 102, 11272–11277.

ten Berge D, Brugmann SA, Helms JA, Nusse R, 2008. Wnt and FGF signals interact to coordinate growth with cell fate specification during limb development. Development 135, 3247–3257. [PubMed: 18776145]

Vaahtokari A, Aberg T, Thesleff I, 1996. Apoptosis in the developing tooth: association with an embryonic signaling center and suppression by EGF and FGF-4. Development 122, 121–129. [PubMed: 8565823]

Vallon V, Platt KA, Cunard R, Schroth J, Whaley J, Thomson SC, Koepsell H, Rieg T, 2011. SGLT2 mediates glucose reabsorption in the early proximal tubule. J Am Soc Nephrol 22, 104–112. [PubMed: 20616166]

Wente W, Efanov AM, Brenner M, Kharitonenkov A, Koster A, Sandusky GE, Sewing S, Treinies I, Zitzer H, Gromada J, 2006. Fibroblast growth factor-21 improves pancreatic beta-cell function

and survival by activation of extracellular signal-regulated kinase 1/2 and Akt signaling pathways. Diabetes 55, 2470–2478. [PubMed: 16936195]

Westphal D, Kluck RM, Dewson G, 2014. Building blocks of the apoptotic pore: how Bax and Bak are activated and oligomerize during apoptosis. Cell Death Differ 21, 196–205. [PubMed: 24162660]

Yin Y, White AC, Huh SH, Hilton MJ, Kanazawa H, Long F, Ornitz DM, 2008. An FGF-WNT gene regulatory network controls lung mesenchyme development. Dev Biol 319, 426–436. [PubMed: 18533146]

Youle RJ, Strasser A, 2008. The BCL-2 protein family: opposing activities that mediate cell death. Nat Rev Mol Cell Biol 9, 47–59. [PubMed: 18097445]

Highlights

- *Fgf8* prevents apoptosis in the cortical nephrogenic progenitors in the kidney
- Blocking apoptosis in Fgf8 mutants rescues loss of cortical nephrogenic progenitors
- Rescue of cortical nephrogenic progenitors does not rescue nephron development
- *Fgf8* is required for Lhx1 expression and subsequent nephron formation

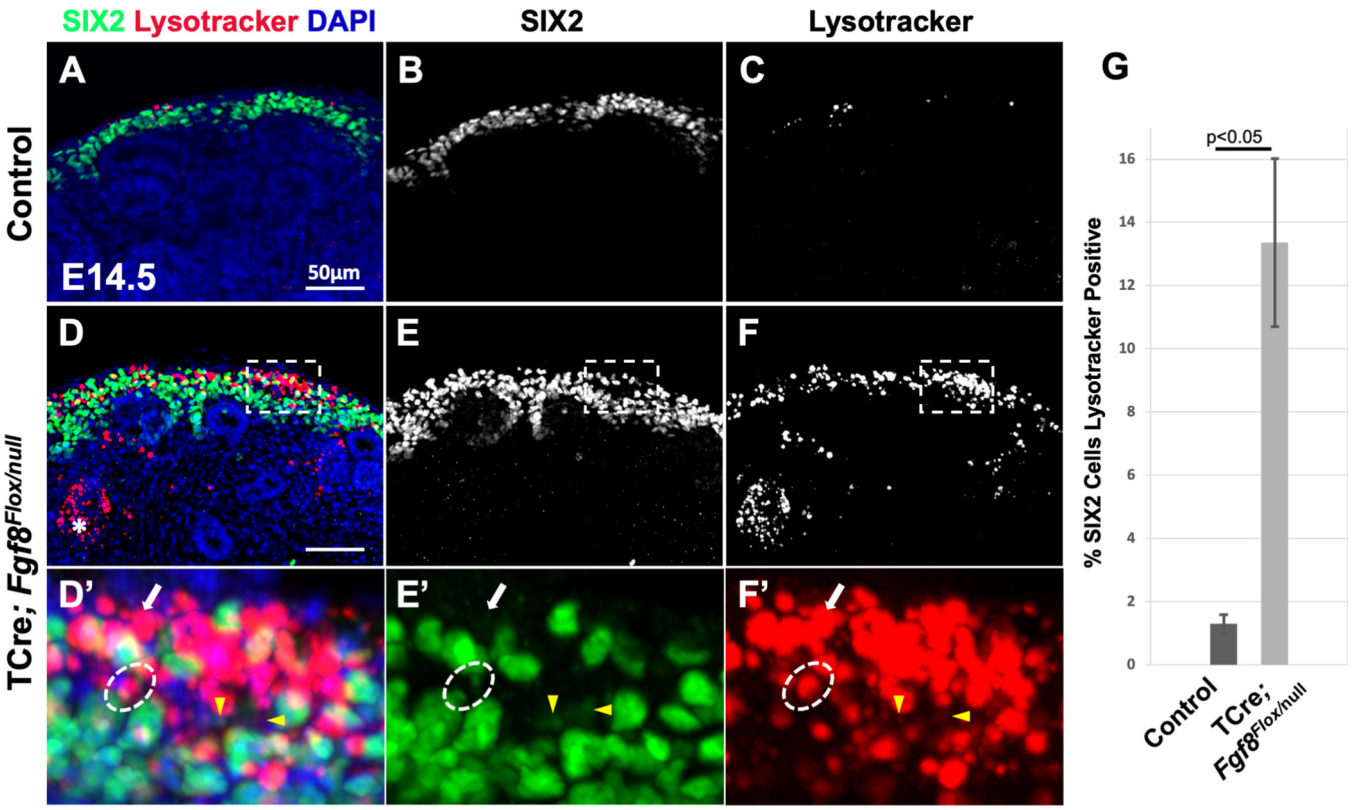

Figure 1 |. Loss of *Fgf8* causes cell death in metanephric mesenchyme progenitors.

A- F') Immunostaining for SIX2 and Lysotracker red staining indicating dying cells in the cortical region of an E14.5 Control and TCre; $Fgf8^{flox/null}$ mutant kidney. Note abundant dying cells in the TCre; $Fgf8^{flox/null}$ mutant kidney (D,F) comparted to very few dying cells in control (A, C). Also note, cell death in renal vesicle (asterisks D). **D'-F')** Region noted by white boxes in D, E and F, showing examples of cells that have low SIX2 and Lysotracker (yellow arrowheads), SIX2 staining closely associated with Lysotracker with minimal overlap (white dashed oval), or Lyostracker and no SIX2 (white arrows). **G)** Quantification of the percentage of SIX2 positive cells that are also lysotracker positive. A-F, max intensity projections of confocal images, ~40um thick mid-sagittal sections; Control n = 6, TCre; $Fgf8^{flox/null}$ n = 4. Error bares represent +/− S.E.M., Student's T-test was used to determine significance.

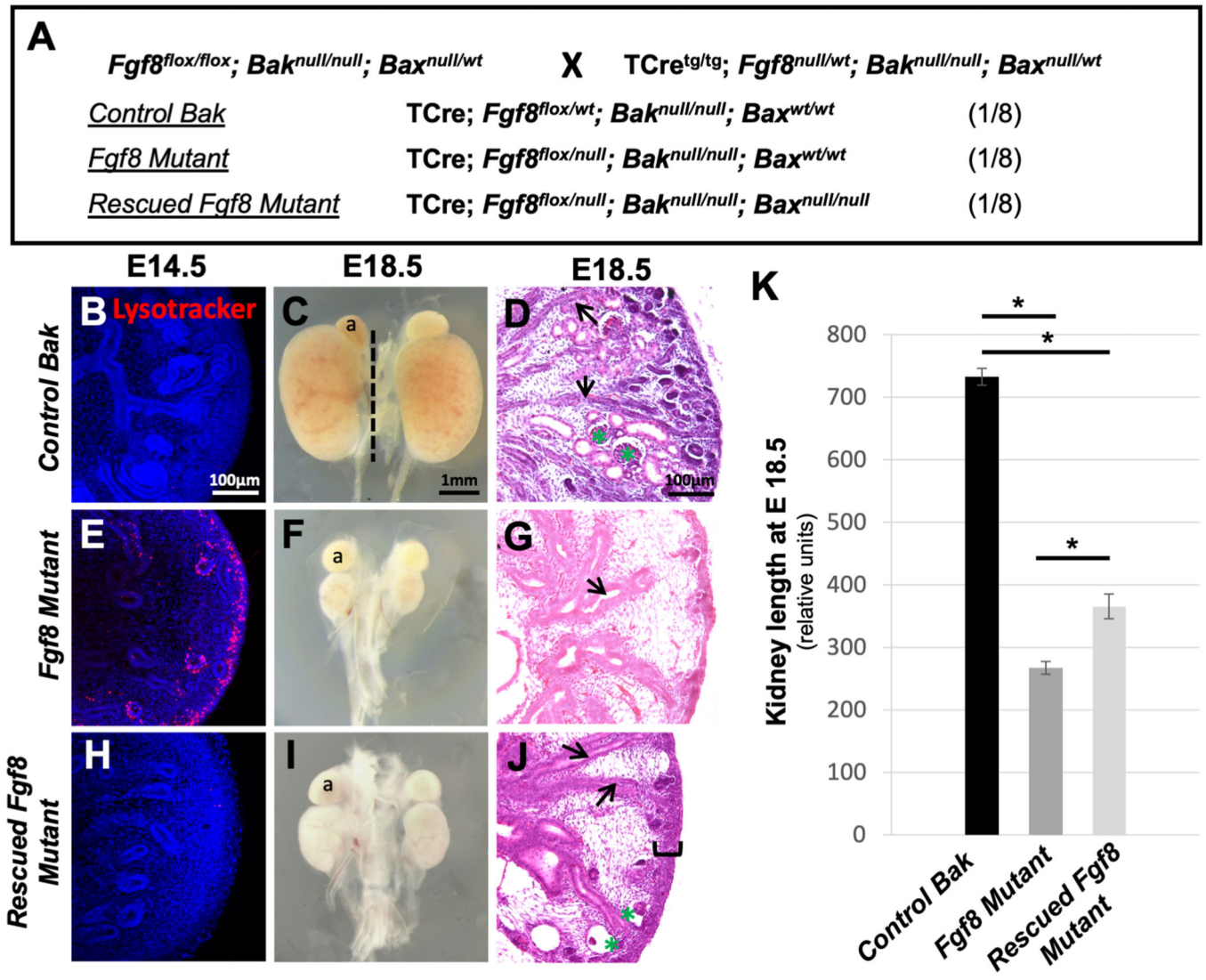

Figure 2 |. Loss of Bak and Bax rescues aberrant cell death in *Fgf8* mutants.

A) Genetic cross to produce the three genotypes of interest listed below with assigned shorthand names (underlined). Note each genotype occurs at a frequency of 1/8; embryos heterozygous for Bax were not analyzed. **B, E, H)** Mid-sagittal sections of lysotracker stained E14.5 kidneys showing cell death; sections are counterstained with DAPI. **C, F, I)** Bright field image of whole E18.5 kidneys. Note, comparative size of adrenal gland (a) and kidney. **D, G, J**) Mid-sagittal thin sections of E18.5 kidneys. Black arrows point to tubules of uretic bud and green asterisks denote glomeruli. **K)** Graph of measurements of the length of E18.5 kidneys. Data represent the average length of the right and left kidney, dotted line in C indicates example of measurement. Error bars represent +/− SEM, Student's t-test was used to determine significance: *$p < 0.05$. n = a minimum of 3 for all images. For K, *Control Bak* n = 6, *Fgf8 Mutant* n = 12, *Rescued Fgf8 Mutant* n = 5.

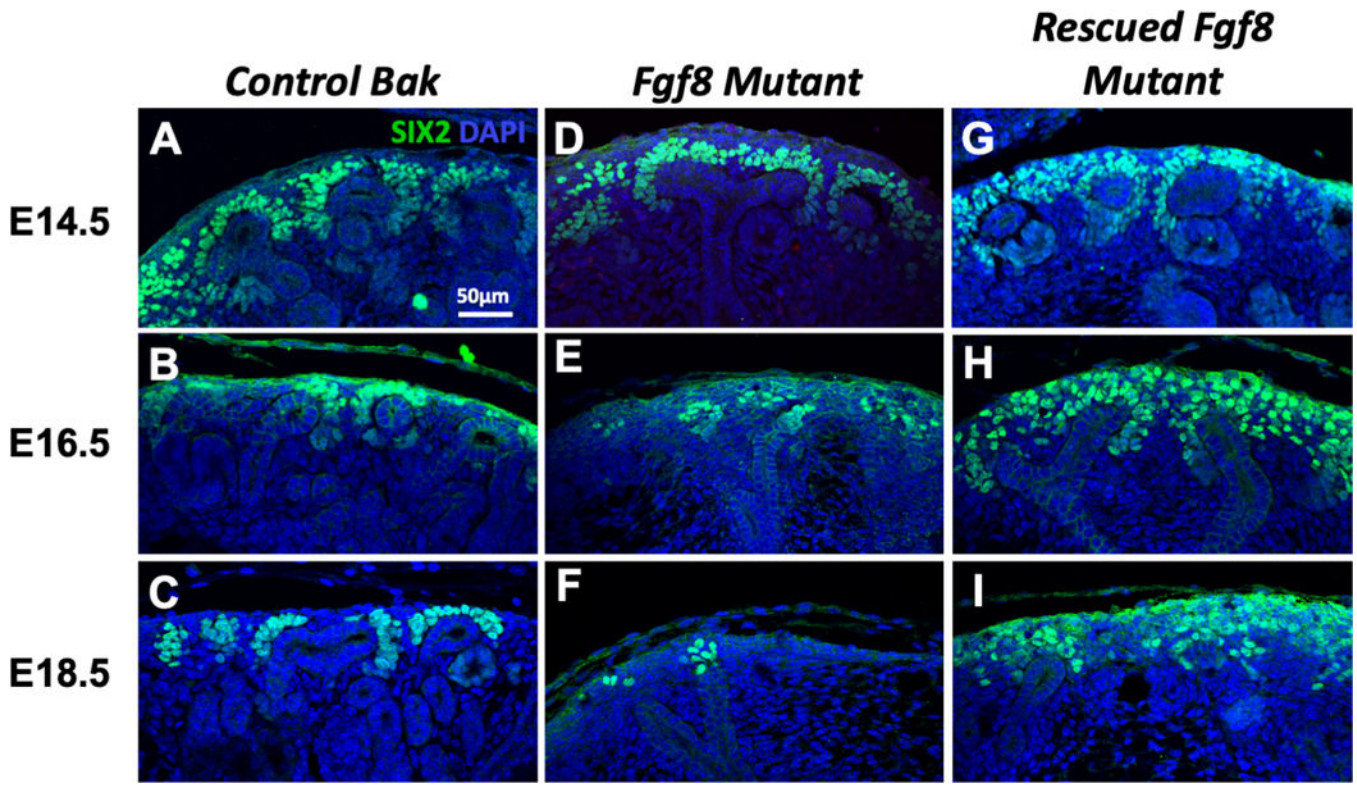

Figure 3 |. Restoring cell survival rescues loss of the Six2 progenitor population.

A-I) Max intensity projections of mid-sagittal sections of SIX2 stained kidneys of noted genotypes at noted stages; sections are counterstained with DAPI. n = a minimum of 3 for all images.

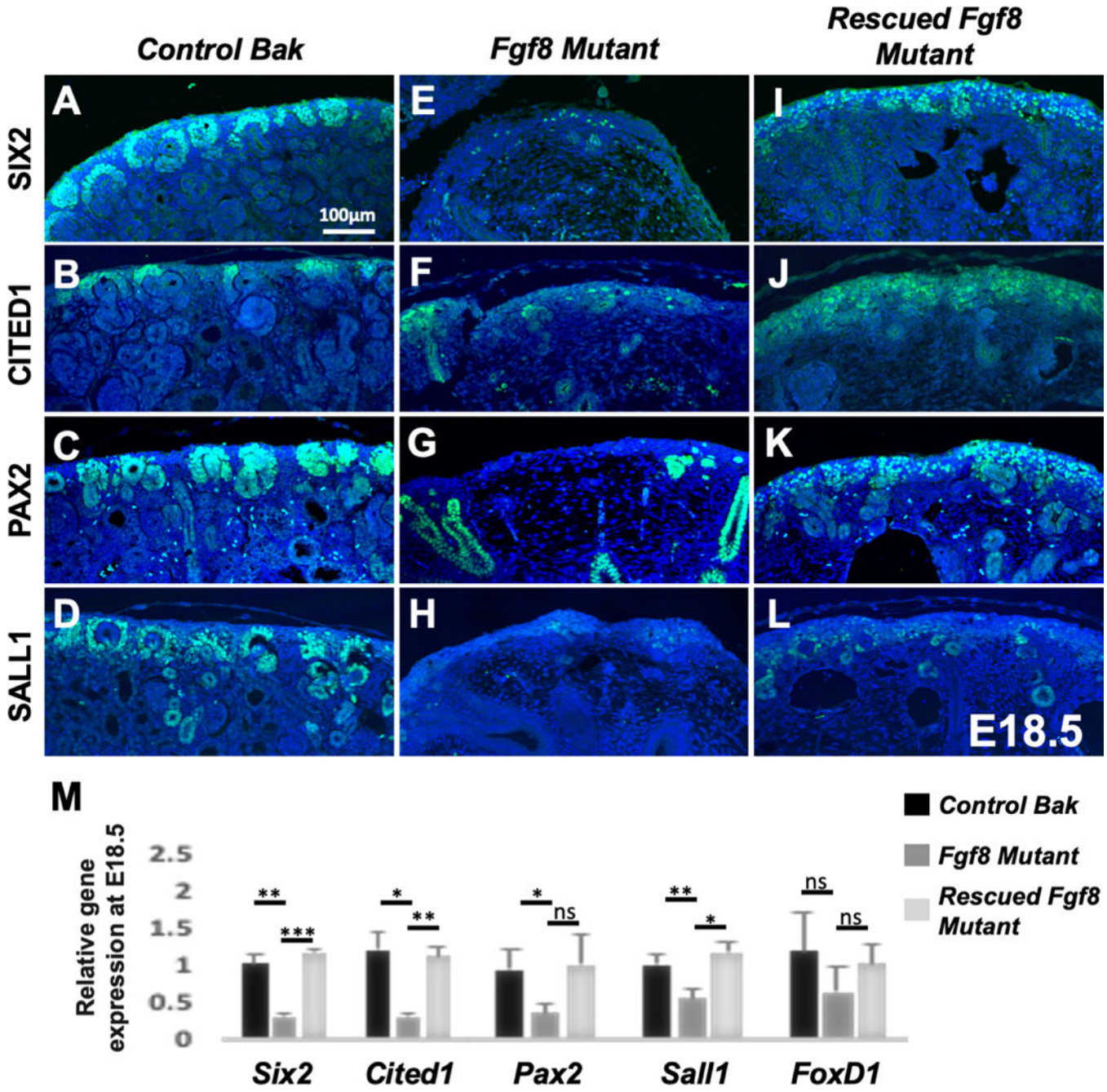

Figure 4 |. Restoring cell survival in *Fgf8* mutants rescues nephron progenitors.

A-L) Max intensity projections of mid-sagittal sections of immunostained embryos for noted markers and genotypes at E18.5. n = a minimum of 3 for all images. **M)** Relative amount of gene expression of noted markers determined by quantitative PCR at E18.5. Error bars represent +/− SEM, Student's t-test was used to determine significance: *p < 0.05, **p < 0.01, ***p < 0.001. n = 3 for genotypes and markers except *Control Bak* analysis for *Pax2* for which n = 6.

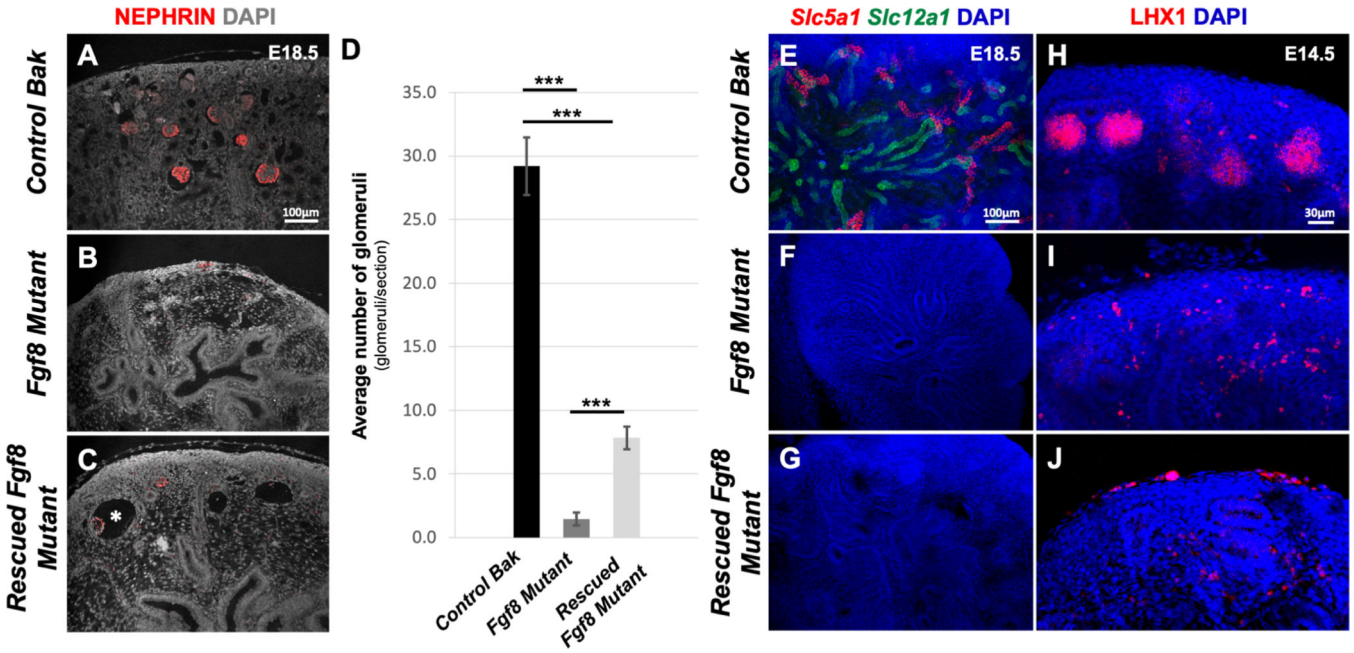

Figure 5 |. Restoring cell survival in *Fgf8* does not rescue nephrogenesis.

A-C) Max intensity projections of mid-sagittal sections of NEPHRIN immunostained kidneys at E18.5. White asterisk in C notes cystic glomerulus. **D)** Quantification of glomeruli counts Error bars represent +/− SEM, Student's t-test was used to determine significance: ***p < 0.001. *Control Bak* n = 5, *Fgf8 Mutant* n = 6, *Rescued Fgf8 Mutant* n = 6. **E-G)** Max intensity projections of mid-sagittal sections of *in situ* hybridization chain reaction (HCR) detection of *Slc5a1* and *Slc12a1* mRNA at E18.5. **H-J)** Max intensity projections of mid-sagittal sections of LHX1 immunostained kidneys at E14.5. n = a minimum of 3 for all images.